



Natural Ventilation in Passive System of Vertical Two-Stores Solar Chimney

Open
Access

Hussein J. Mohammed^{1,*}, Abbas J. Jubear¹, Haddi Obaid¹

¹ Department of Mechanical Engineering, Wasit University, Kut, Iraq

ARTICLE INFO

ABSTRACT

Article history:

Received 9 January 2020
Received in revised form 6 February 2020
Accepted 7 February 2020
Available online 18 April 2020

The present work includes a numerical study that investigated in a thermal performance of the passive system of a vertical two stores solar chimney. A several models of a vertical solar chimneys were designed, by using the solid work 18 software, that then brought to the Ansys Fluent 18.2 software for simulation, under (Al-Kut, Iraq) city climatic conditions on the hot summer day of (5-8-2018). This simulation was comprised of a five testing models of a two stores solar chimney that oriented to the south and equipped with a wooden two stores facility building that having the size of (1 * 1 * 1) m³ for each store. The testing models includes a vertical and long vertical solar chimney, with two different positions of (lower and upper) inlet holes. The testing was aimed to choosing the perfect model that could giving a suitable thermal performance under a various value of solar intensities and ambient temperatures during a constant interval of the daylight times. The results proved that the long vertical solar chimney was able to providing a best natural ventilation but with visible rising into the indoor temperatures.

Keywords:

Two stores solar chimney; Thermal performance; Natural ventilation; CFD; ACH

Copyright © 2020 PENERBIT AKADEMIA BARU - All rights reserved

1. Introduction

The solar chimney is a passive implement that benefit from the solar radiation, for ventilating the indoor space. It had converting the heating energy into the kinetic by means of a free convection concept. This operation occurred due to the buoyancy effect, that generates due to heating the absorber part of the solar chimney and thereby causing the temperature difference between the inner higher temperature of the solar chimney and the lower temperature of the indoor space. The buoyancy operation could generate the upward air flow through the system and causing then the indoor ventilation that represented by the ACH.

Many previous studies were dealing with the thermal performance of the solar chimneys. Sompop *et al.*, [1] studied numerically and experimentally the thermal performance of the long

* Corresponding author.

E-mail address: omaxshopping@gmail.com (Hussein J. Mohammed)

vertical solar chimney (that equipped with a three stores testing building model of the size $(1.2 * 2 * 1) \text{ m}^3$ for each store) and the other same model of a three stores building that does not equipped with a solar chimney. The study occurred under the mild climatic states of Bangkok and it showed that the three stores solar chimney model [that having a one top outlet hole and a three inlet holes (one for each store)] was the best, by reducing the indoor temperature with $(4 \sim 5) \text{ C}^\circ$, relying on the store height consequently. Soubhi and Waleed [2] were researching experimentally the effects of the vertical chimney orientation, chimney height, number of chimneys and chimney air gap width, on the indoor natural ventilation. The results showed that the using of the south direction, long height vertical solar chimney, number of vertical solar chimney and low width air gap solar chimney, would giving the best results with a higher ventilation and low indoor temperatures, whereas using a two and a three chimneys would rising the indoor ventilation with 13% and 33% respectively. While using the one, two and three solar chimneys would reduce the indoor temperature with 6%, 10% and 12% sequently. Abbas and Ali [3] investigated by a numerical study the influence of utilizing the solar chimney for improving the indoor natural ventilation. These studies were occurred in (Al-Kut, Iraq) city on a June day, by testing a variform types of a solar chimneys that deals with a chimney numbers, chimney orientation and chimney inclination angle, under the effects of the solar intensities and ambient temperatures during a constant interval of the daytimes. The results showed that using of the two solar chimneys (one towards south and one towards west), the south direction and 45° inclination angle, were giving a good result of a natural ventilation that represented by ACH. Hussain and Yit [4] analyzed with experimental study the natural ventilation of three testing design of a vertical and horizontal rooftop solar chimneys. The first model was containing a vertical absorber panel with two holes of (the system top outlet and the room lower inlet). While, the second model was containing a vertical and a horizontal absorbers panels with three holes of (the system top outlet and the room lower inlet, adding to the hole of the ambient horizontal panel). The third model was containing a two vertical absorbers panels with two holes of (the system top outlet and the room lower inlet). The results showed that the third model was the best ones by giving a good air ventilation with 1.2% and 7.6% comparing with the results of the first and second models respectively, due to the increasing of the absorber areas that would causing in rising the buoyancy force. Alex and Nyuk [5] searched experimentally the natural ventilation of the Zero Energy Building (ZEB) that consist of three stores with a vertical solar chimney, under a hot-humid climate of Singapore. The results showed that the solar chimney was able to enhancing the indoor space with 0.49 m/s of maximum air speed and the interior temperature would be being higher at first but it decreasing step by step with about 1-2 hour comparing with the other buildings in the region. Moreover, the inlet hole position of the classroom store of the first store solar chimney affected significantly into the indoor ventilation and the lowering suitable position may reaching the interior air speed to the maximum value of 0.6 m/s . Insaf and Nouredine [6] studied by the Fluent CFD simulation the effect of using the solar chimney on the indoor natural ventilation that represented by ACH. This study was depending on some parameters that affected directly into the buoyancy effects such as solar intensities and chimney air gap width. The solar intensities were the main factor that affected significantly on ACH and the optimum ACH was relying on the air gap width ratio. While, the maximum ACH was obtained by $(0.2 \sim 0.3) \text{ m}$ of the air gap width. Hakim *et al.*, [7] investigated on the power plant of (a horizontal solar chimney and a suitable collector entrance), for reducing the electricity consumptions especially in deserts regions. It was fulfilling by a numerical study of a 2D axisymmetric chimney, by taking into account the effects of the collector entrance (slope, sloping distance) on the air thermo-hydrodynamic demeanor that thereby influenced on the system performance. The results showed that the collector entrance shape was affected visibly on the system performance and the collector configuration of $(9.1^\circ$ slope, 0.8 sloping distance) could

producing a power of 16.36 % more than zero slope collector. Moreover, it is also showed that the optimal slope would depending on the sloping distance under a different Rayleigh numbers examined. Ali Asghar *et al.*, [8] presented a numerical study of the solar chimney power plant under the influent of the solar intensity, pressure drop of turbine and the soil porosity. The system could construct on the soil surface with a several specifications and porosities, for using as a layer of energy storage. The soil porosity that effected on the solar chimney output power was searched, for choosing the optimal one. The results showed that the solar chimney output power might depending on the turbine pressure drop under each solar intensity and soil porosity. It also showed that the increasing in the solar intensity would producing the increases in the turbine output power with decreasing in the solar chimney efficiency and the land of the less porosity and high solar intensity could be the optimal for giving the best results. Nguyen and Wells [9] were searched by the CFD simulation, the thermal performance of the solar chimney (that having a horizontal absorber plate). The testing had been including the effects of some parameters of (solar intensity, absorber surface length, chimney air gap length and the width and height of the chimney inlet and outlet sections) on the amount of the induced air flow rate that passing through the chimney air gap. Ahmed Abdeen *et al.*, [10] studied numerically and experimentally the optimizing design of the solar chimney, for enhancing the indoor natural ventilation that induced by the natural convection air flow, in Egypt houses. The numerical study had achieved by the CFD simulation that validated with the experimental testing. The results showed, that the inclined solar chimney dimensions of (75° inclination angle, 2.65 m width, 0.28 m air gap, 1.85 m height) would giving the optimizing indoor air speed of (0.28, 0.47, 0.52) m/s, at the actual solar intensities of (500, 700 and 850) W/m² respectively. Moreover, the optimal results might depend on the solar chimney parameters of (width, inclination angle and the air gap) sequently. Nadia *et al.*, [11] investigated numerically (by CFD simulation), the coupled cooling passive system of the inclined solar chimney (45°) with the EAHE. They had coupled with (1 * 1 * 1) m³ testing room, for enhancing the system thermal performance in (a dry and semi dry) Algeria weathers. The results revealed that the EAHE of (40 ~ 45) m length and 2.5 m depth, was able by assist of (8 W) fan to debase the indoor temperature with (8 C°) even when the ambient temperature and the solar intensity might exceed the values (39 C° and 700 W/m²) respectively. Moreover, the (1 * 0.35) m² solar chimney was able to creating the ACH visibly depending on solar intensities. Kinan and Che Sidik [12] searched experimentally the using of a circular and square collector designs (SUTPP), with the dimensions of (1.5 m and 0.08 m PVC tower length and diameter, respectively; adding to 3.14 m² of collector area). It which considered as an alternative way for generating the electricity power from solar radiation energy, in the developing countries, especially in the rural regions. A solar intensity, ambient temperature and the tower indoor velocity, were recorded every one hour during 4 days and they represented the main parameters that could affected on (SUTPP) performance. The results showed that the circular design was the perfect ones, by giving a higher indoor tower temperature and velocity; while the maximum values obtained at 3:00 pm.

2. Study Aims

In the hot climate countries such as Iraq, the time periods of using the conventional ventilation and cooling equipment would being higher a long day, especially in summer season. It means more consumption of the electricity, that would cost a heavy expensive and may causing a risk of environmental pollution. The alternative solution would represent by using the air conditioning passive systems that exploiting the renewable energies such as solar radiation, geothermal, water fallen and others, energies. Therefore, due to the heavy solar incident during the summer that

accesses 900 W/m^2 , the suitable alternative passive energy would be being the solar radiation energy, that benefit from it by using the solar chimney instrument for enhancing the buildings ventilation naturally.

3. CFD Simulation Analysis

The computational fluid dynamic simulation has been including many analytical sequent steps, as geometrical design, meshing generation, governing equations and the assumptions of the boundary conditions. The comparison between the obtaining results and the other previous studies (that dealing with the same conditions of this CFD simulation), were discussed then by validation.

3.1 Geometrical Design

The present study was comprised of four models of a vertical solar chimneys, that consist of the same construction materials and the same orientation of the south direction, as shown in Figure 1 to Figure 5. All these models were equipped to the vertical two stores building prototype, that having the similar store size of $(1 * 1 * 1) \text{ m}^3$. The first and the second model's dimensions were (1 m width, 0.3 m depth and 2.041 m height), while the third and the fourth model's dimensions were (1.008 m width, 0.3 m depth and 3.016 m height). The 3D models design was fulfilling by the Solid Work 18 software and then brought to the Ansys Fluent 18.2 for completing the others simulation steps. The solar chimneys were made from a black absorber of aluminium panel with (1 mm) thickness and a three faces of a glass panes, that surroundings the absorber panel to configures the solar chimney air gap [3]. While, the two stores building were made from a wood of (8mm) thickness, the roof insulator of (25 mm) thickness and the other insulator that covered the vertical southern wall with (50 mm) thickness [3]. Each store of the building owns the $(0.3 * 0.3) \text{ m}^2$ inlet window, that situated in the mid of the northern wall, as shown in Figure 5. In addition, each store would be having the $(1 * 0.3) \text{ m}^2$ solar chimney inlet hole, that located in the upper or lower position of the southern wall, depending on the model type.

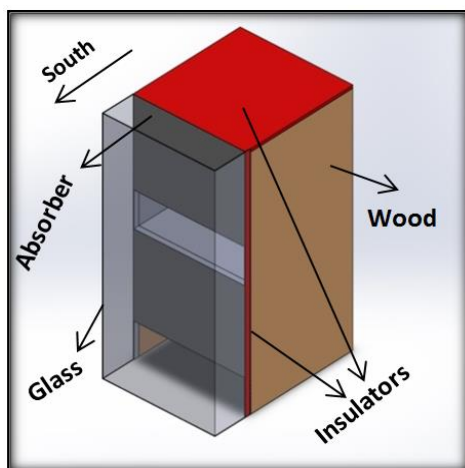


Fig. 1. The first geometry model

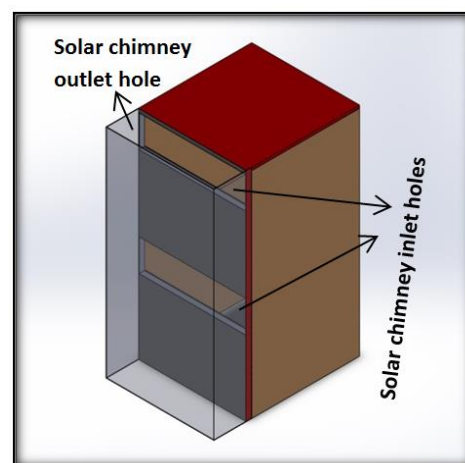


Fig. 2. The second geometry model

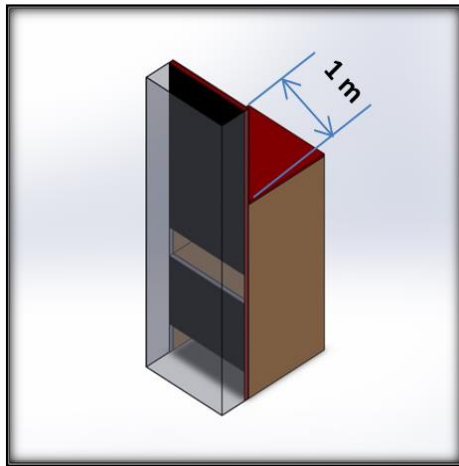


Fig. 3. The third geometry model

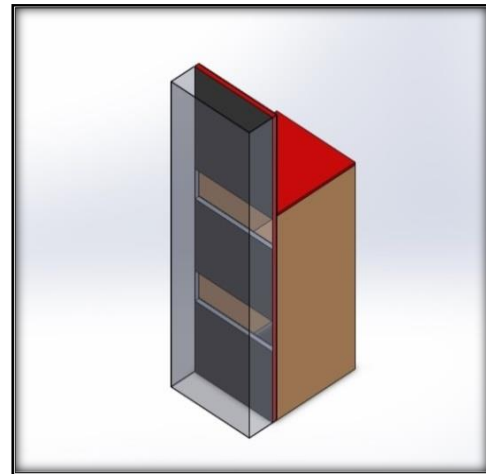


Fig. 4. The fourth geometry model

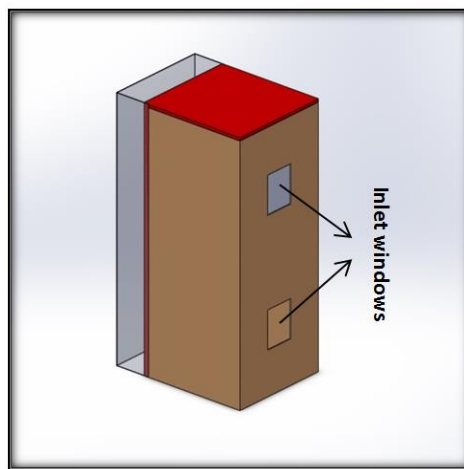


Fig. 5. Building inlet holes

Table 1 have been shown the thermal specifications of the system constructions materials [3].

Table 1

Thermal properties of construction materials

n	Materials	Thickness (mm)	Density (ρ) Kg/m ³	Specific heating (Cp) Kj/kg.k	Thermal conductivity (K) W/m.k	Absorptivity (α)	Emissivity (ϵ)	Transitivity (T)
1	Glass	4	2220	0.83	1.15	0.06	0.95	0.84
2	Aluminum	1	2700	0.9	273	0.95	0.95	0
3	Wood	8	400	1.8	0.06	0.5	0.5	0
4	Insulator	50, 25	52	0.657	0.038	0.4	0.4	0

3.2 Meshing Generation

The accuracy of the simulation results could mainly depend on the meshing state, by dividing the system's body into a number of control cells. The regular precise meshing will be giving more accuracy, for the predicting results of the flow heat transfer behaviors. It would rely on the mesh distribution lines and their intensity. This study has been used a two different meshing types of a tetrahedron and a hexahedron with a high meshing cells number, access to 11 million cells, as shown in the Figure 6.

After achieved a several meshing attempts for choosing the optimal mesh that should giving a good ACH, the best choice was comprised of 11,576,962 elements (via a suitable PC processor with a short time). It occurred through the third model of the long vertical solar chimney at 14:00 pm and its properties and details would mention in the Table 2 and Table 3 respectively, whereas the first store ACH was 10.805 and the second store 10.098.

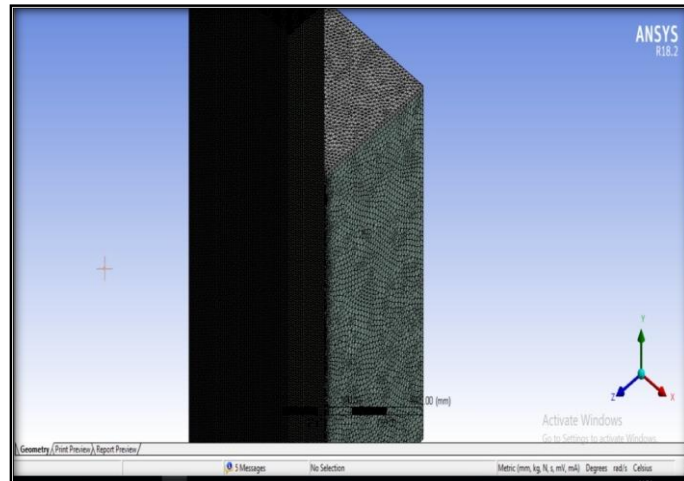


Fig. 6. The mesh generation

Table 2
 The optimum meshing properties

Total elements	11576962	
Total nodes	2141415	
Tetrahedron	Element = 10928668	Node = 2097351
Hexahedron	Element = 648294	Node = 44064
Relevance	0	
Relevance center	Fine	
Size function	Curvature	
Max face size	7 mm	
Max tet size	14 mm	
Growth rate	1.2	
Smoothing	High	
Mesh metric	Aspect ratio	
	min	average
	1.15	1.86

Table 3
 The optimum meshing details

n	Domains	Tetrahedron	Hexahedron	Elements	Nodes
1	Air		0	9822271	1853453
2	Wood		0	145665	50902
3	Insulator			1441098	289495
4	Absorber	0		50316	102220
5	Glass	0		108612	216000

3.3 Governing Equations

A two types of (3D) flow equations were used in the ANSYS FLUENT 18.2 to solving the air and the solar radiation behaviors by a free convection of the heat transfer concept. Therefore, the governing equations were divided into two different portions as air flow equations and solar radiation transfer equation (RTE).

3.3.1 Air flow equations

This equations were comprised of a (3D) turbulent equations of (continuity, momentum and energy).

Continuity Equation:

$$\frac{\partial U}{\partial x} + \frac{\partial V}{\partial y} + \frac{\partial W}{\partial z} = 0 \quad (1)$$

Momentum Equations:

X- Direction

$$\rho \left[U \frac{\partial U}{\partial x} + V \frac{\partial U}{\partial y} + W \frac{\partial U}{\partial z} \right] = -\frac{\partial p}{\partial x} + \frac{\partial}{\partial x} \left[\mu \frac{\partial U}{\partial x} - \overline{\rho u' u'} \right] + \left[\frac{\partial}{\partial y} \left[\mu \frac{\partial U}{\partial y} - \overline{\rho u' v'} \right] + \frac{\partial}{\partial z} \left[\mu \frac{\partial U}{\partial z} - \overline{\rho u' w'} \right] \right] + S_U \quad (2)$$

Y- Direction

$$\rho \left[U \frac{\partial V}{\partial x} + V \frac{\partial V}{\partial y} + W \frac{\partial V}{\partial z} \right] = -\frac{\partial p}{\partial y} + \frac{\partial}{\partial x} \left[\mu \frac{\partial V}{\partial x} - \overline{\rho u' v'} \right] + \left[\frac{\partial}{\partial y} \left[\mu \frac{\partial V}{\partial y} - \overline{\rho v' v'} \right] + \frac{\partial}{\partial z} \left[\mu \frac{\partial V}{\partial z} - \overline{\rho v' w'} \right] \right] + S_V \quad (3)$$

Z- Direction

$$\rho \left[U \frac{\partial W}{\partial x} + V \frac{\partial W}{\partial y} + W \frac{\partial W}{\partial z} \right] = -\frac{\partial p}{\partial z} + \frac{\partial}{\partial x} \left[\mu \frac{\partial W}{\partial x} - \overline{\rho u' w'} \right] + \left[\frac{\partial}{\partial y} \left[\mu \frac{\partial W}{\partial y} - \overline{\rho v' w'} \right] + \frac{\partial}{\partial z} \left[\mu \frac{\partial W}{\partial z} - \overline{\rho w' w'} \right] \right] + S_W \quad (4)$$

Energy Equation:

$$\rho \left[U \frac{\partial T}{\partial x} + V \frac{\partial T}{\partial y} + W \frac{\partial T}{\partial z} \right] = \frac{\partial}{\partial x} \left[\frac{\mu}{\sigma_T} \frac{\partial T}{\partial x} - \overline{\rho u' t'} \right] + \left[\frac{\partial}{\partial y} \left[\frac{\mu}{\sigma_T} \frac{\partial T}{\partial y} - \overline{\rho v' t'} \right] + \frac{\partial}{\partial z} \left[\frac{\mu}{\sigma_T} \frac{\partial T}{\partial z} - \overline{\rho w' t'} \right] \right] \quad (5)$$

3.3.2 Solar Radiation Transfer Equation (RTE)

For absorb, dissipating and emitting the side \vec{r} to moving towards the \vec{s} direction, the (RTE) were used here as

$$\frac{dI(\vec{r}, \vec{s})}{ds} + (a + \sigma_s) I(\vec{r}, \vec{s}) = a n^2 \frac{\sigma T^4}{\pi} + \frac{\sigma_s}{4\pi} \int_0^{4\pi} I(\vec{r}, \vec{\xi}) \Phi(\vec{s}, \vec{\xi}) d\Omega' \quad (6)$$

3.4 Assumptions of The Boundary Conditions

There were some hypotheses had been used in the present work for simplifying the CFD simulation solving and prevent any more losing of the solution data.

- i. 3D Steady turbulent flow.
- ii. Incompressible Newtonian viscous fluid.
- iii. Boussinesq air density.
- iv. Constant air properties of (c_p , k , ρ , ν).

The present work occurred under the experimental climatic data of Al-Kut city of the (5-8-2018) day with a constant intervals hours (8:00 am to 18:00 pm), as shown in the Table 4 [13].

As shown in the Figure 7, the boundary conditions were including a several assuming states that planning in advance for fulfilling the CFD simulation solutions carefully.

- i. Using the inlet and outlet pressures method with the atmospheric zero gage and its ambient temperature.
- ii. The size of each store is $(1 * 1 * 1) \text{ m}^3$ and it made from opaque wooden walls.
- iii. The vertical solar chimney is made from a semi-transparent panes of glass and a black aluminum absorber panel. All surfaces are in a parallel situation and in a constant temperatures.
- iv. The air flow on the solid system walls would being in NO slip state and the velocity is equal to zero on the surfaces.
- v. Using the (K- ϵ) turbulence model with a standard wall functions.
- vi. Using the discrete ordinate (DO) model in the solar radiation solvers.
- vii. All the system walls are exchanging the heat with conduction, convection and radiation concepts.

Table 4
Climatic data Of Al-Kut city of (5-8-2018) day

n	Hour	Solar Radiation (W/m^2)	Ambient Temperature (K)	Relative Humidity (%)	Wind Speed m/s
1	8:00	480	312	23	1.6
2	10:00	710	317	18	2.77
3	12:00	875	320	13	2.77
4	14:00	725	320	13	4.44
5	16:00	410	319	11	6.38
6	18:00	100	318	12	6.2

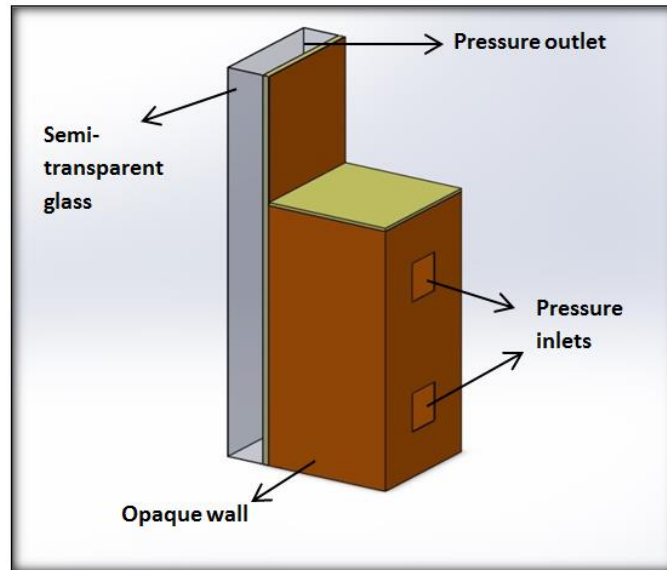


Fig. 7. Boundary condition states

4. Validation of The CFD Simulation

The first CFD simulation with south orientation model of Ali and Abbas [13] was taking into accounts for validating the present work results under the same construction models but at the climatic conditions of (5-8-2018) [13]. The validation results showed a good concordance with 5.71% of the average error percentage of the ACH, depending on the solar intensity and the ambient temperature during the daylight times, as shown in the Figure 8.

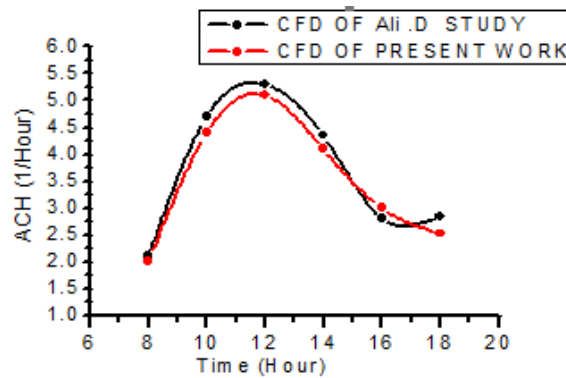


Fig. 8. Comparison of CFD simulations

5. Results and Discussions

Figure 9 and Figure 10 show the solar intensity and the ambient temperature behaviors during the daylight times (8:00 am to 18:00 pm) of the (5-8-2018) day, whereat they being rising step by step until reaching the hour of 12:00 am and then reducing sequently till the hour of 18:00 pm.

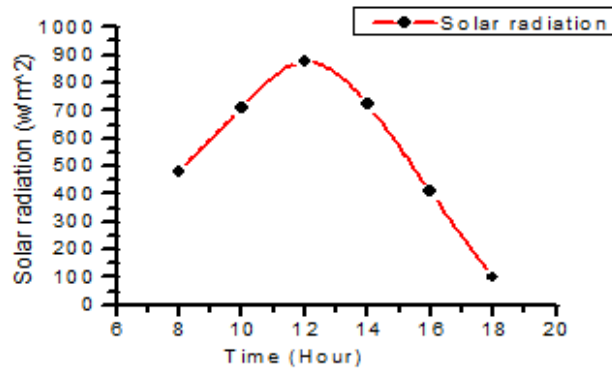


Fig. 9. Solar radiation intensity of (5-8-2018) daylight times

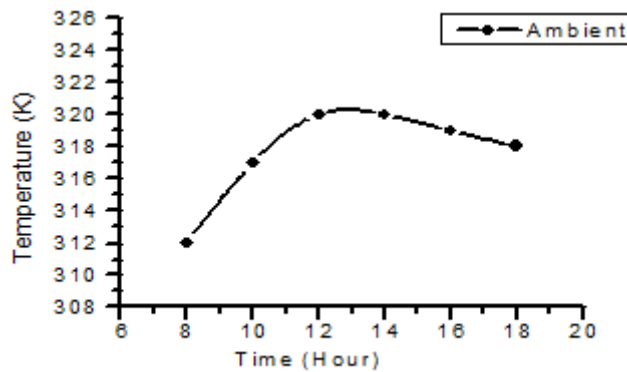


Fig. 10. Ambient temperatures of (5-8-2018) daylight times

As the solar intensity and the ambient temperature are effecting directly on the indoor thermal performance, they would considered as the main factors that would effecting on the present study, by enables the passive system from generating the ACH that would action on the indoor temperatures visibly.

5.1 CFD Simulation Results

The present study were including four testing models of a two-stores vertical solar chimneys that they would effected directly by the solar intensities, ambient temperatures, chimney height and the inlet chimney holes. The testing purpose was to obtaining the suitable model that could giving a good ACH. All the velocity vectors and temperature contours that shown in the operation actions were selected at the mid- section of the system body, because the maximum flow would happen the visible results.

The results showed that the ACH stores and the indoor stores temperatures would being rising according to the solar intensities and ambient temperatures rising and vise-versa. It showed that the maximum ACH would occurred at 14:00 pm with the maximum indoor temperatures for each store. While, the minimum ACH would occurred at the 18:00 pm with the minimum indoor temperatures at 8:00 am for each store. The ACH of the first store would having a higher values than the second store, due to the vertical constructions of the models, that could depending on the chimney air gap height and thereby rising from the second store temperature and being rather than the first store

during the daylight times. In all four models testing, the results showed that the indoor stores temperatures values would being more than the ambient temperatures.

5.1.1 Result of the first model

As shown in Figure 1, the first model is comprised of a vertical solar chimney with a lower inlet holes of $(1 * 0.3) \text{ m}^2$ for each store. Figure 11 and Figure 12 show the ACH and the indoor temperatures of the two stores, wherent the maximum ACH was 9.477 and it occurred at 14:00 pm in the first store with the maximum second store temperature of 336.17 K. The minimum ACH was 1.56 and it occurred at 18:00 pm in the second store with the minimum first store temperature of 318.56 K that occurred at 8:00 am. Figure 13 and Figure 14 show the velocity vector and the temperature contour of the maximum state at 14:00 pm.

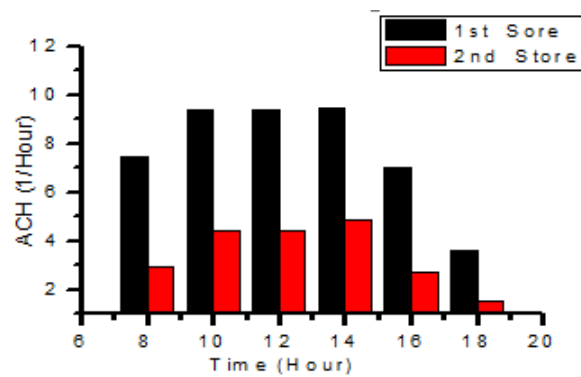


Fig. 11. The first model ACH stores

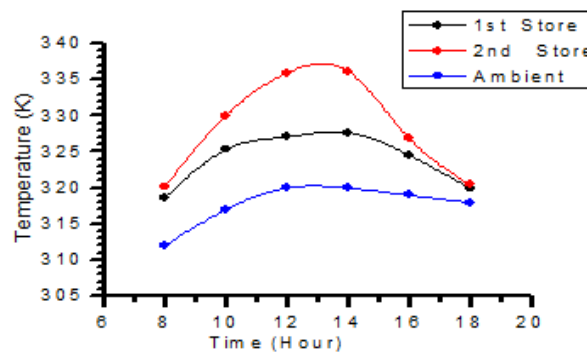


Fig. 12. The first model stores temperatures

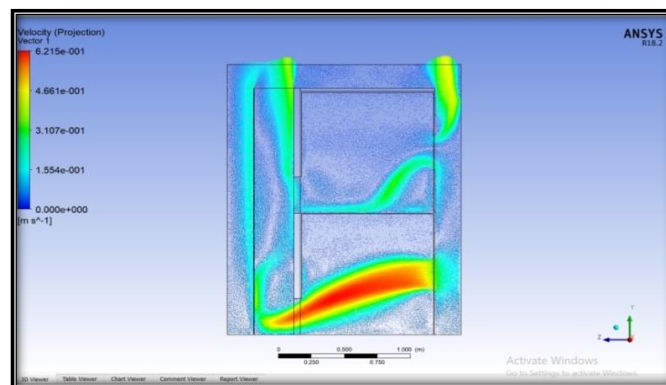


Fig. 13. The first model velocity vector at maximum state

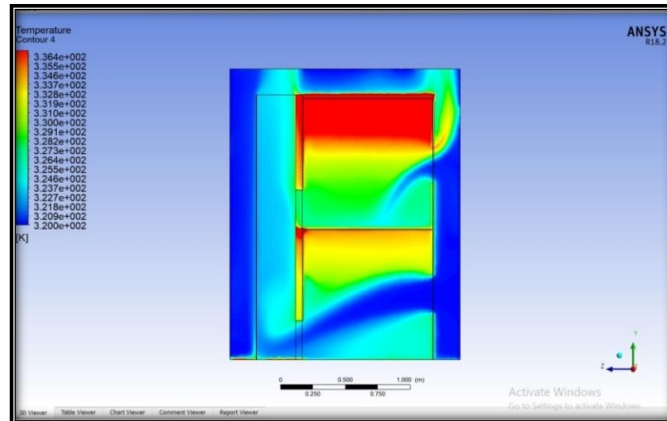


Fig. 14. The first model temperature contour at maximum state

5.1.2 Result of the second model

The second model is exactly similar to the first model but the inlet holes located on the upper part of the southern wall in each store with the same previous dimensions, as shown in Figure 2. Figure 15 and Figure 16 show the ACH and the indoor temperatures of the two stores, where at the maximum ACH was 6.93 and it occurred at 14:00 pm in the first store with the maximum second store temperature of 325.06 K. The minimum ACH was 1.77 and it occurred at 18:00 pm in the second store with the minimum first store temperature of 314.51 K that recorded at 8:00 am. Figure 17 and Figure 18 show the velocity vector and the temperature contour of the maximum state at 14:00 pm.

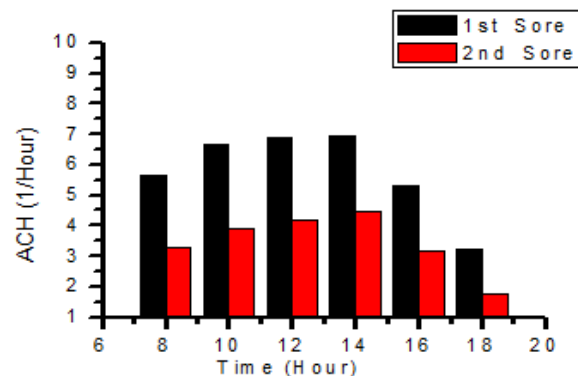


Fig. 15. The second model ACH stores

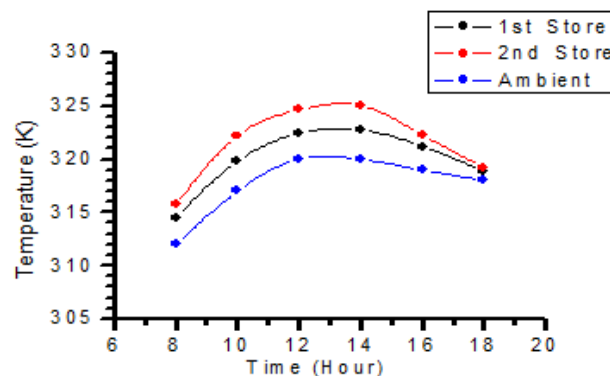


Fig. 16. The second model stores temperatures

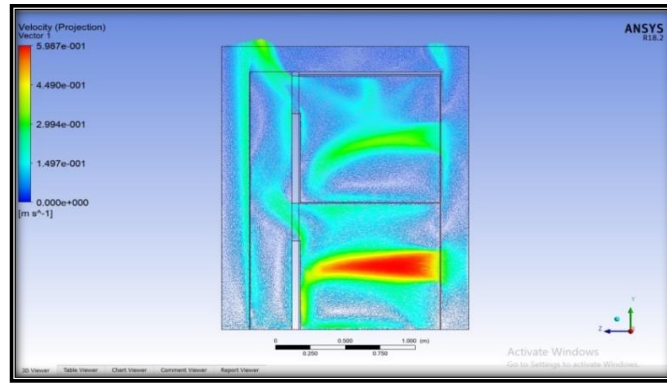


Fig. 17. The second model velocity vector at maximum state

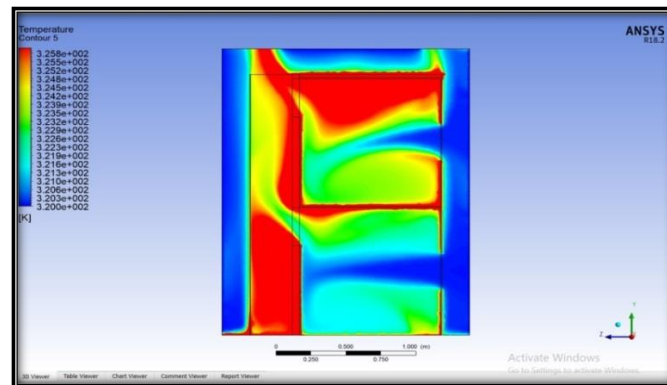


Fig. 18. The second model temperature contour at maximum state

5.1.3 Result of the third model

The third model have been including a long vertical solar chimney, as shown in Figure 3, with a lower inlet holes of $(1 * 0.3) \text{ m}^2$ for each store. Figure 19 and Figure 20 showed the ACH and the indoor temperatures of the two stores, whereat the maximum ACH was 10.805 and it occurred at 14:00 pm in the first store with the maximum second store temperature of 331.321 K. The minimum ACH was 4.167 and it occurred at 18:00 pm in the second store with the minimum first store temperature of 318.53 K that occurred at 8:00 am. Figure 21 and Figure 22 shown the velocity vector and the temperature contour of the maximum state at 14:00 pm.

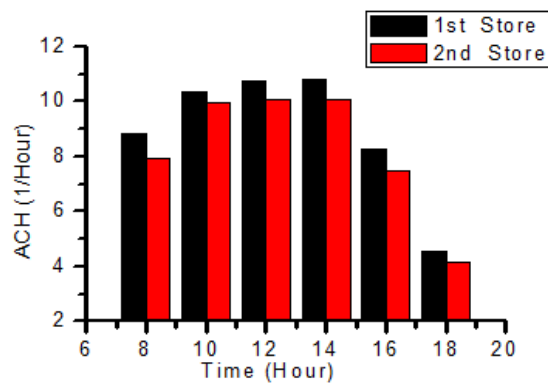


Fig. 19. The third model ACH stores

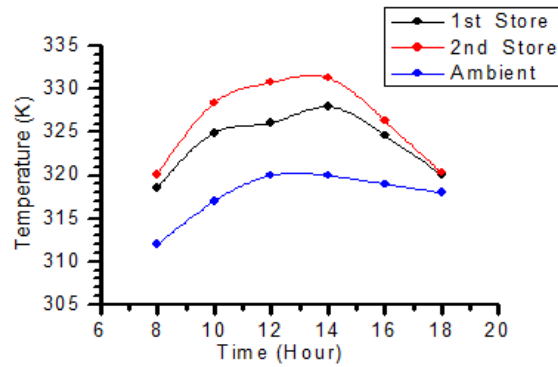


Fig. 20. The third model stores temperatures

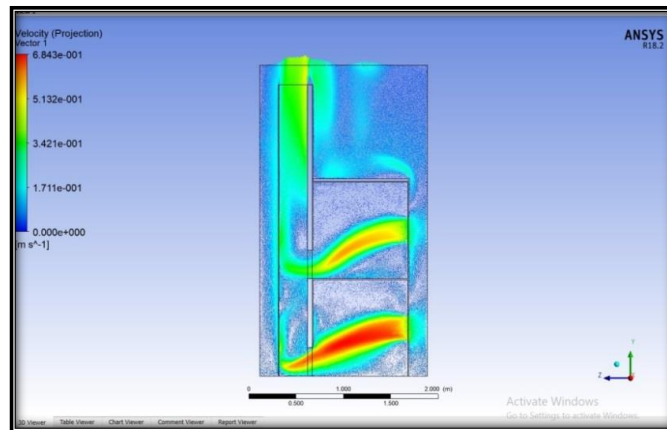


Fig. 21. The third model velocity vector at maximum state

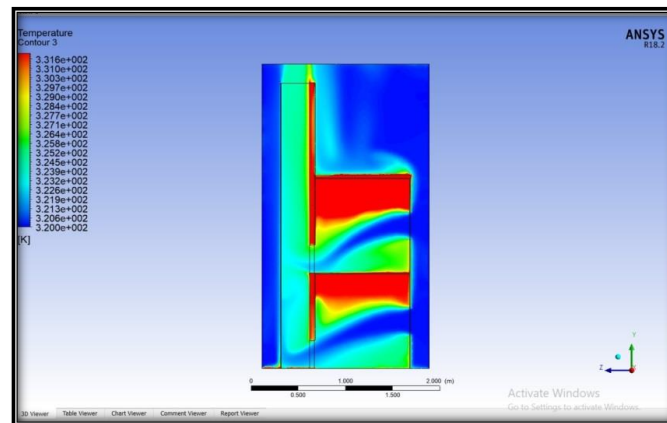


Fig. 22. The third model temperature contour at maximum state

5.1.4 Result of the fourth model

The fourth model is exactly similar to the third model but the inlet holes located on the upper part of the southern wall in each store with the same previous dimensions, as shown in Figure 4. Figure 23 and Figure 24 show the ACH and the indoor temperatures of the two stores, whereat the maximum ACH was 8.29 and it occurred at 14:00 pm in the first store, with the maximum second store temperature of 323.63 K. The minimum ACH was 3.12 and it occurred at 18:00 pm in the second

store, with the minimum first store temperature of 314.13 K that occurred at 8:00 am. Figure 25 and Figure 26 show the velocity vector and the temperature contour of the maximum state at 14:00 pm.

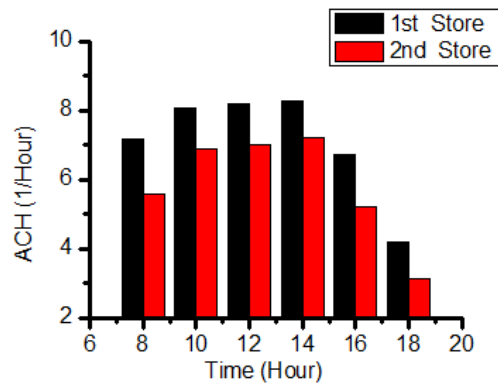


Fig. 23. The fourth model ACH stores

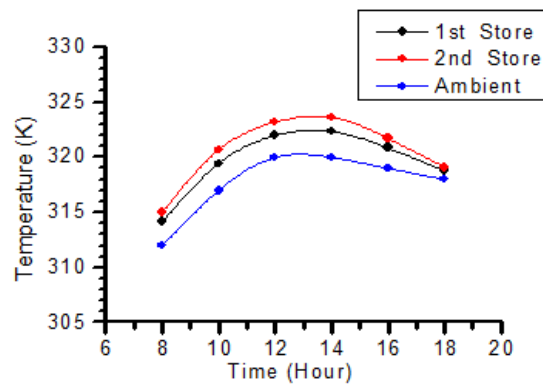


Fig. 24. The fourth model stores temperatures

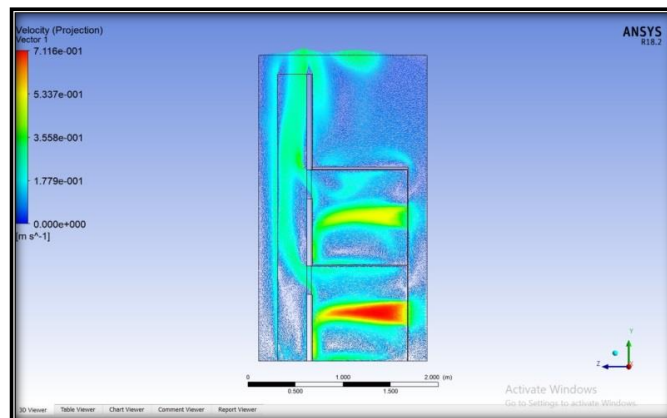


Fig. 25. The fourth model velocity vector at maximum state

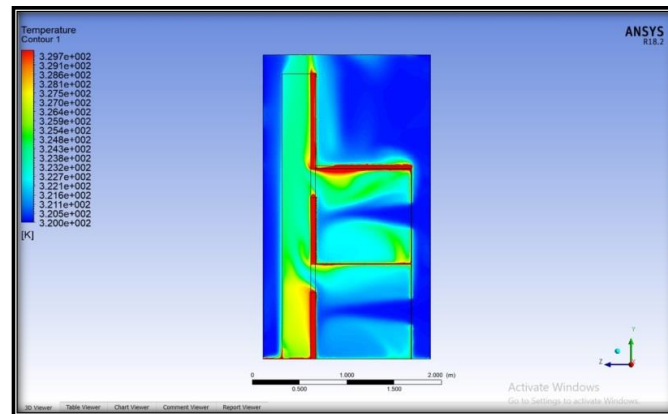


Fig. 26. The fourth model temperature contour at maximum state

6. Conclusions

The maximum average ACH for the passive four models, during the daylight times, was (8.93 for first store, 8.29 for second store) and it occurred in the third model. The minimum average ACH for the passive four models, during the daylight times, was (5.78 for first store, 3.45 for second store) and it occurred in the second model.

The maximum average indoor temperatures for the passive four models, during the daylight times, was (323.85 K for first store, 328.27 K for second store) and it recorded in the first model. The minimum average indoor temperatures for the passive four models, during the daylight times, was (319.59 K for first store, 320.54 K for second store) and it recorded in the fourth model.

The average ambient temperatures and the average solar radiation intensities that recorded during the daylight times of (5-8-2018) day were 317.66 K and 550 W/m² respectively and thereby, the comparison would seem the visible rising of the average's indoor stores temperatures.

The highest ACH value was occurred in the first store of the third model at 14:00 pm. The lowest ACH value was occurred in second store of the first model at 18:00 pm. The highest indoor temperature value was recorded in the second store of the first model at 14:00 pm. The lowest indoor temperature value was recorded in the first store of the fourth model at 8:00 am.

The passive system of the vertical solar chimney can be using perfectly in the mild climates with a low wind speed, while in a hot- dry climates it could rise the indoor temperatures visibly, as mentioned in the present study. In the hot-dry climates the vertical solar chimney can be using with the other passive cooling system that coupled with it together, as (the earth air tunnel heat exchanger), that would reduce from the indoor temperatures and enhancing the indoor thermal performance perfectly. The docile vertical constructions of the passive system would enable the Architects from using this invention in the residential fields in future.

References

- [1] Punyasompun, Sompop, Jongjit Hirunlabh, Joseph Khedari, and Belkacem Zeghmati. "Investigation on the application of solar chimney for multi-storey buildings." *Renewable Energy* 34, no. 12 (2009): 2545-2561. <https://doi.org/10.1016/j.renene.2009.03.032>
- [2] Hassanein, Soubhi A., and Waleed A. Abdel-Fadeel. "Improvement of natural ventilation in building using multi solar chimneys at different directions." *Journal of Engineering Sciences* 40, no. 6 (2012): 1661-1677.
- [3] Jubear, Ass Prof Dr Abbas J., and Ali Dhahi Ghareer. "Numerical Investigations on Solar Chimney Inclination Angle for Room Ventilation." *International Journal of Engineering & Technology* 7, no. 4.17 (2018): 1-9.
- [4] Al-Kayiem, Hussain H., and Yit Man Heng. "Experimental investigation of rooftop solar chimney for natural ventilation." *Journal of Engineering and Applied Sciences* 10 (2015): 10249.

- [5] Tan, Alex Yong Kwang, and Nyuk Hien Wong. "Natural ventilation performance of classroom with solar chimney system." *Energy and Buildings* 53 (2012): 19-27.
<https://doi.org/10.1016/j.enbuild.2012.06.010>
- [6] Mehani, Insaf, and Nouredine Settou. "Passive cooling of building by using solar chimney." *World Academy of Science, Engineering and Technology International Journal of Civil, Environmental, Structural, Construction and Architectural Engineering* 6, no. 9 (2012): 735-736.
- [7] Kebabsa, Hakim, Mohand Said Lounici, Mohamed Lebbi, and Ahmed Daimallah. "Thermo-hydrodynamic behavior of an innovative solar chimney." *Renewable Energy* 145 (2020): 2074-2090.
<https://doi.org/10.1016/j.renene.2019.07.121>
- [8] Sedighi, Ali Asghar, Zeynab Deldoost, and Bahram Mahjoob Karambasti. "Effect of Thermal Energy Storage Layer Porosity on Performance of Solar Chimney Power Plant Considering Turbine Pressure Drop." *Energy* (2019): 116859.
<https://doi.org/10.1016/j.energy.2019.116859>
- [9] Nguyen, Y. Q., and J. C. Wells. "A numerical study on induced flowrate and thermal efficiency of a solar chimney with horizontal absorber surface for ventilation of buildings." *Journal of Building Engineering* 28 (2020): 101050.
<https://doi.org/10.1016/j.jobbe.2019.101050>
- [10] Abdeen, Ahmed, Ahmed A. Serageldin, Mona GE Ibrahim, Abbas El-Zafarany, Shinichi Ookawara, and Ryo Murata. "Solar chimney optimization for enhancing thermal comfort in Egypt: An experimental and numerical study." *Solar Energy* 180 (2019): 524-536.
<https://doi.org/10.1016/j.solener.2019.01.063>
- [11] Saifi, Nadia, Nouredine Settou, Belkheir Negrou, and Abdessamia Hadjadj. "Design and functional analysis of earth- air heat exchanger (EAHE) coupled with solar chimney in South East Algeria." *Academia Journal of Scientific Research* 5, no. 12 (2017): 732-744.
- [12] Kinan, A., and N. A. Che Sidik. "Experimental studies on small scale of solar updraft power plant." *Journal of Advanced Research Design* 22, no. 1 (2016): 1-12.
- [13] Dhahi, Ali, and Ass Prof Dr Abbas J. Jubear. "Numerical and Experimental Investigation of The Ventilation Performance of a Building with Multi-Solar Chimneys." Degree of Master of Science in Mechanical Engineering's Thesis, Wasit University, 2019.